DOI: 10.1002/ejic.200501141

Syntheses and Fluxional Processes of Diphenyl(2-thienyl)phosphane Derivatives of Triosmium Clusters

Nitsa K. Kiriakidou Kazemifar,[a] Marc J. Stchedroff,[a] M. Abdul Mottalib,[a][‡] Simona Selva,[b] Magda Monari,[b] and Ebbe Nordlander*[a]

Keywords: Cluster / Thienylphosphane / Fluxionality / Hydrodesulfurisation

Thermal treatment of $[Os_3(CO)_{12}]$ with diphenyl(2-thienyl)phosphane, $Ph_2P(C_4H_3S)$, results in the formation of $[Os_3(CO)_{12-x}\{Ph_2P(C_4H_3S)\}_x]$ (x = 1–3, **1**–**3**), but no C–H bond activation was observed. Reaction of $[H_2Os_3(CO)_{10}]$ with diphenyl(2-thienyl)phosphane at ambient temperature affords $[HOs_3(\mu\text{-}H)(CO)_{10}\{Ph_2P(C_4H_3S)\}]$ (**4**), but when the same reaction is repeated at elevated temperatures, the cyclometallated species $[(\mu\text{-}H)Os_3(CO)_9\{\mu_3\text{-}Ph_2P(C_4H_2S)\}]$ (**5**) and $[(\mu\text{-}H)Os_3(CO)_8\{\mu_3\text{-}Ph_2P(C_4H_2S)\}\{Ph_2P(C_4H_3S)\}]$ (**6**) are formed. In addition, two more products, tentatively assigned as $[(\mu\text{-}H)Os_3(CO)_6\{\mu_3\text{-}Ph_2P(C_4H_2S)\}\{\mu\text{-}Ph_2P(C_4H_3S)\}\{Ph_2P(C_4H_3S)\}]$ (**7**) and $[(\mu\text{-}H)Os_3(CO)_7\{\mu\text{-}Ph_2P(C_4H_2S)\}\{\mu\text{-}Ph_2P(C_4H_3S)\}\{Ph_2P(C_4H_3S)\}]$ (**8**) are obtained. The dynamic behaviours of **2**, **5** and **6** have been studied by variable-temperature (VT) ^1H and $^{31}P\{^1H\}$ NMR spectroscopy. The VT $^{31}P\{^1H\}$ NMR spectra of $[Os_3(CO)_{10}\{Ph_2P(C_4H_3S)\}_2]$ (**2**) demonstrate that a mixture of two isomers, which are in rapid exchange at room temperature, is present and that the less common *cis-trans* isomer, whose structure has been determined by X-ray crystallography, is favoured for this cluster. The VT ^1H NMR spectra of **5** indicate the presence of two isomers which are proposed to arise from an oscillation of the σ,η^2-vinyl group of the thienyl moiety between two metal atoms. A similar fluxional process is proposed to occur in **6** and the assignment of the room-temperature structure(s) of this cluster was confirmed by $^1H\text{-}^{187}Os$ 2D HMQC spectroscopy. In addition to **2**, the solid-state structures of **3**, **5** and **6** have been determined by X-ray crystallography.

Introduction

More strict laws concerning sulfur-containing emissions have intensified the interest in hydrodesulfurisation (HDS) processes. As a consequence, studies of adsorption and activation of organosulfur compounds onto metal surfaces is a rapidly developing area. The objectives of this research are the understanding of the nature of the active HDS catalysts, the binding modes and the activation of sulfur-containing molecules – in particular thiophenes – at the active catalyst sites, and the improvement of the efficiency of the catalysts.[1–6] Organometallic complexes,[3–5] including transition-metal clusters,[7] have been used as models for HDS catalysts because mechanistic information easily can be extracted by spectroscopic and analytical studies of discrete molecular complexes.

One of the very first reports of the interaction of thiophene with organometallic compounds described the desulfurisation of the heterocycle by a metal cluster, $[Fe_3(CO)_{12}]$.[8,9] Rauchfuss and co-workers[10] demonstrated shortly after, that thiaferroles are easily converted into the corresponding ferroles on heating and thereby established that insertion of an iron atom into a C–S bond clearly activates the heterocycle towards desulfurisation [Scheme 1(a)]. Similarly, the reaction of $[Ru_3(CO)_{12}]$ with thiophene proceeds through C–S bond cleavage, producing the sulfur-free ferrole-type compound $[Ru_2(\mu\text{-}C_4H_4)(CO)_6]$ and the tetranuclear cluster $[Ru_4(\mu_3\text{-}S)(\mu\text{-}C_4H_4)(CO)_{11}]$;[11] this is the first reported example of desulfurisation of a thiophene in which both the extruded sulfur and the hydrocarbon residue remain coordinated within the same complex [Scheme 1(b)]. More recently, Angelici and co-workers[12] have demonstrated $[Re_2(CO)_{10}]$-promoted C–S bond cleavage in benzothiophenes.

Despite the above-mentioned examples of C–S bond activation, C–H bond activation predominates over other types of oxidative addition in reactions of thiophenes with $[M_3(CO)_{12}]$ (M = Ru, Os) and their derivatives.[7] Thus, the carbonyltriosmium clusters $[Os_3(CO)_{12}]$ and $[Os_3(CO)_{10}(MeCN)_2]$ react with thiophene and thiophene derivatives through C–H bond cleavage in preference to C–S bond cleavage to afford the *endo*- and *exo*-thienyl isomers of

---

[a] Inorganic Chemistry, Center for Chemistry and Chemical Engineering, Lund University,
Box 124, 22100 Lund, Sweden
Fax: + 46-46222-4439
E-mail: Ebbe.Nordlander@inorg.lu.se
[b] Dipartimento di Chimica "G. Ciamician", Università degli Studi di Bologna,
via Selmi 2, 40126 Bologna, Italy
[‡] On leave from: Bangladesh College of Leather Technology, Hazaribagh, Dhaka 1209, Bangladesh

Supporting information for this article is available on the WWW under http://www.eurjic.org or from the author.

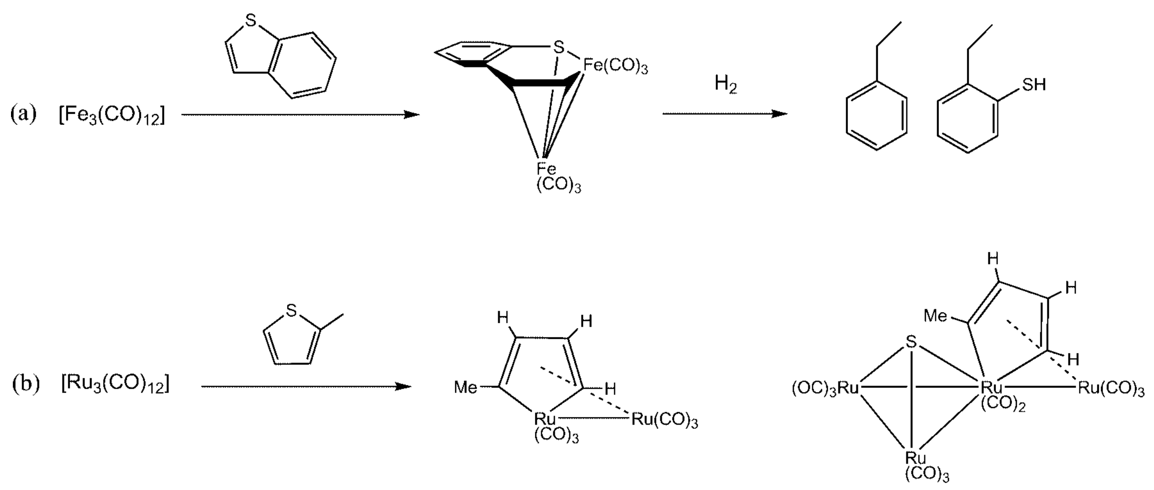

Scheme 1. Examples of desulfurisation of benzothiophene and 2-methylthiophene by carbonyl transition-metal clusters (see text and references cited therein).

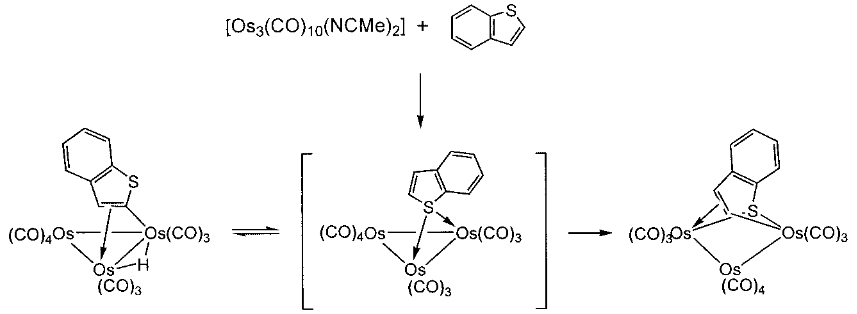

Scheme 2. Room-temperature C–S bond cleavage effected by a carbonyltriosmium cluster (cf. ref.[17]).

$[Os_3(\mu\text{-}H)(CO)_9(\mu\text{-}C_4H_2S)]$, which are in rapid equilibrium at room temperature.[13–15] Similar results have been observed for 2-methylthiophene, 2,2′-bithiophene and 2,2′:5′,2′′-terthiophene.[16] The first room-temperature C–S bond cleavage of a (benzo)thiophene coordinated to a metallic cluster was reported by Arce et al.[17] In chloroform at room temperature the cluster $[Os_3(\mu\text{-}H)(CO)_{10}(\mu\text{-}C_8H_5S)]$, which contains a μ-η^2-benzothienyl ligand, undergoes C(vinyl)–S bond cleavage to yield the cluster $[Os_3(CO)_{10}(\mu\text{-}C_8H_6S)]$, which contains an open benzothiophene ligand coordinated to an open Os_3 unit through a μ-S atom and a μ-η^2-vinyl group (Scheme 2).

Despite the above-mentioned examples of thiophene coordination and activation, thiophene remains a relatively poor ligand for low-valent metal complexes, and thienylphosphanes [e.g. diphenyl(2-thienyl)phosphane] have therefore been used to bring the heterocycle into the coordination sphere of transition-metal clusters through the phosphane moiety of the ligand.[18–20] Treatment of diphenyl(2-thienyl)phosphane with $[Ru_3(CO)_{12}]$ has led to the incorporation of the thiophene ring into tri- and tetraruthenium clusters by cyclometallation and C–P bond cleavage of the ligand.[20] Here we report the reactions of $[Os_3(CO)_{12}]$ and $[H_2Os_3(CO)_{10}]$ with diphenyl(2-thienyl)phosphane, $Ph_2P(C_4H_3S)$, which have been undertaken in an effort to achieve C–P and C–S bond cleavage of the ligand.

Results and Discussion

Thermal Treatment of $[Os_3(CO)_{12}]$ with $Ph_2P(C_4H_3S)$

Reaction of $[Os_3(CO)_{12}]$ with diphenyl(2-thienyl)phosphane, $Ph_2P(C_4H_3S)$, in refluxing toluene yielded, after separation by thin layer chromatography, three yellow, substituted compounds, which were identified as $[Os_3(CO)_{11}\{PPh_2(C_4H_3S)\}]$ (**1**) (23%), $[Os_3(CO)_{10}\{PPh_2(C_4H_3S)\}_2]$ (**2**) (44%), and $[Os_3(CO)_9\{PPh_2(C_4H_3S)\}_3]$ (**3**) (8%) on the basis of their IR spectra. They are analogous with those of known mono-, bis-, and tris(phosphane)-substituted triosmium clusters.[21–24] The FAB mass spectra of all three compounds are also in complete agreement with the proposed formulas.

The ^1H NMR spectra of **1**–**3** display only aromatic resonances. No hydrido signals could be detected, indicating that *ortho*-metallation had not taken place. The room-temperature $^{31}P\{^1H\}$ NMR spectra show a singlet at δ = –16.2 ppm for **1**, a signal at δ = –17.3 (br.) ppm and doublet at δ = –32.7 ($J_{P\text{–}P}$ = 6.4 Hz) ppm for **2** (vide infra), and a singlet at δ = –17.2 ppm for **3**. The $^{31}P\{^1H\}$ spectra of both **1** and **3** remain unchanged when the temperature is decreased to –60 °C. This is consistent with the presence of one isomer of both **1** and **3**, in which the phosphane ligand(s) adopt equatorial positions with respect to the cluster. However, the low-temperature $^{31}P\{^1H\}$ NMR spectrum of **2** indicates the presence of more than one isomer. The two most reasonable isomers are the *cis-trans* and *trans-trans* isomers (*cis* or *trans* with respect to the Os–Os vector) shown in Figure 1, which have previously been detected for related $[Os_3(CO)_{10}(phosphane)_2]$ clusters.[25,26] The $^{31}P\{^1H\}$ NMR spectrum at –60 °C (Figure 1) reveals that the predominant form is the *cis-trans* isomer with non-equivalent phosphorus nuclei, represented by two singlets at δ = –18.12 and –21.97 ppm.

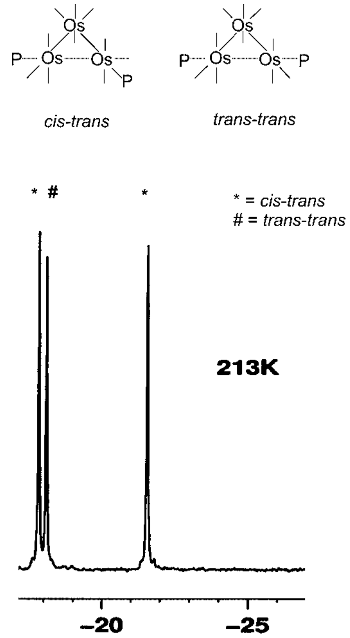

Figure 1. $^{31}P\{^1H\}$ NMR spectrum (CD_2Cl_2, 300 MHz) of $[Os_3(CO)_{10}(Ph_2PC_4H_3S)_2]$ (**2**) at –60 °C. The appearance of two equally intense singlets (δ = –18.12 and –21.97 ppm) is consistent with the *cis-trans* isomer and the third singlet (δ = –18.26 ppm) is attributed to the *trans-trans* isomer.

Until recently, only the *trans-trans* form of an $[Os_3(CO)_{10}(phosphane)_2]$ cluster had been verified crystallographically. Leong and Liu[27] have reported the first crystallographic confirmation of a *cis-trans* structure, that of *cis-trans*-$[Os_3(CO)_{10}(PPh_3)_2]$, which can be crystallised in both isomeric forms. We were able to grow yellow crystals of compound **2** by slow concentration of a dichloromethane/*n*-hexane solution at 4 °C, and these crystals were somewhat surprisingly found to contain only the *cis-trans* isomer. The molecular structure of **2** is shown in Figure 2; selected bond lengths and angles are listed in Table 1.

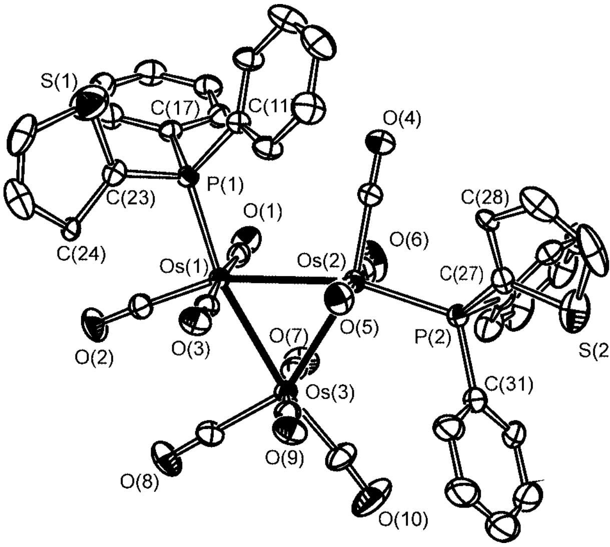

Figure 2. Molecular structure of $[Os_3(CO)_{10}\{Ph_2P(C_4H_3S)\}_2]$ (**2**) (thermal ellipsoids at 30% probability). The carbon atoms of the carbonyl ligands bear the same numbering as the oxygen atoms. Hydrogen atoms have been omitted for clarity.

Table 1. Selected bond lengths [Å] and angles [°] for $[Os_3(CO)_{10}(Ph_2PC_4H_3S)_2]$ (**2**).

Os(1)–Os(2)	2.9104(7)	Os(1)–C(1)	1.946(7)
Os(1)–Os(3)	2.8860(8)	Os(1)–C(2)	1.887(6)
Os(2)–Os(3)	2.9072(6)	Os(1)–C(3)	1.932(6)
Os(1)–P(1)	2.343(2)	Os(2)–C(4)	1.884(6)
Os(2)–P(2)	2.333(2)	Os(2)–C(5)	1.948(7)
P(1)–C(11)	1.847(3)	Os(2)–C(6)	1.918(7)
P(1)–C(17)	1.825(3)	Os(3)–C(7)	1.947(7)
P(1)–C(23)	1.828(6)	Os(3)–C(8)	1.920(7)
P(2)–C(27)	1.820(6)	Os(3)–C(9)	1.951(7)
P(2)–C(31)	1.851(4)	Os(3)–C(10)	1.885(7)
P(2)–C(37)	1.833(4)		
C(1)–Os(1)–C(3)	174.9(2)	P(2)–Os(2)–Os(3)	104.46(4)
C(2)–Os(1)–C(3)	92.6(3)	C(4)–Os(2)–Os(1)	99.1(2)
P(1)–Os(1)–C(2)	96.0(2)	C(4)–Os(2)–Os(3)	156.3(2)
P(1)–Os(1)–Os(2)	106.49(4)	C(7)–Os(3)–C(9)	173.0(3)
P(1)–Os(1)–Os(3)	166.48(4)	C(8)–Os(3)–C(10)	99.6(3)
C(2)–Os(1)–Os(2)	157.1(2)	C(8)–Os(3)–Os(1)	90.9(2)
C(5)–Os(2)–C(6)	178.5(3)	C(8)–Os(3)–Os(2)	151.2(2)
P(2)–Os(2)–C(4)	97.9(2)	C(10)–Os(3)–Os(1)	169.4(2)
P(2)–Os(2)–Os(1)	162.55(4)	C(10)–Os(3)–Os(2)	109.2(3)

The molecule consists of a triangle of osmium atoms with ten carbonyl ligands, four bonded to Os(3) and three to each of Os(1) and Os(2). Two diphenyl(2-thienyl)phosphane ligands occupy equatorial coordination sites on Os(1) and Os(2), respectively. The average Os–Os distance [2.901(1) Å] is slightly longer than that found in the parent cluster, $[Os_3(CO)_{12}]$ [$Os–Os_{ave}$ = 2.877(3) Å].[28] In agreement with previous studies indicating that the presence of a tertiary phosphane ligand tends to lengthen the *cis*-Os–Os bond in $[Os_3(CO)_{11}(phosphane)]$ clusters,[29,30] some lengthening of the Os(1)–Os(2) and Os(2)–Os(3) interactions in *cis* position is observed [2.910(1) and 2.907(1) Å, respectively, vs. Os(1)–Os(3) 2.886(1) Å]. This trend confirms the similar lengthening of the two Os–Os distances in *cis* position in the *cis-trans* form of the cluster $[Os_3(CO)_{10}(PPh_3)_2]$.[27] On the other hand, in *trans-trans* structures of $[Os_3(CO)_{10}(phosphane)_2]$ [phosphane = PPh_3, $PPh(OMe)_2$, $P(OMe)_3$] there is no change of Os–Os bond lengths that can be related to the presence of two phosphane ligands.[31] The Os(1)–P(1) (2.343 Å) and Os(2)–P(2) [2.333(2) Å] distances are normal and close to those reported for $[Os_3(CO)_{10}(PPh_3)_2]$.[27] (*cis-trans* and *trans-trans* forms) and the phosphane-substituted compounds mentioned above. The phosphorus atoms are slightly displaced out of the Os_3 plane [P(1) +0.102(1) and P(2) +0.292(1) Å]. This structure determination and the above-mentioned low-temperature NMR measurements indicate that the *cis-trans* isomer of **2** is the thermodynamically favoured compound, as has previously been found by Deeming and co-workers for related clusters.[25,26]

Compound **3** crystallises with two independent molecules, which are conformational isomers (vide infra), in the asymmetric unit. The molecular structure of **3** is similar to that of previously characterised trisubstituted complexes of the general formula $[M_3(CO)_9(\text{phosphane})_3]$ [M = Os, Ru and phosphane = $PMe_2(CH_2Ph)$, PMe_2Ph, $PPh(OMe)_2$, $P(OEt)_3$, $P(OCH_2CF_3)_3$ and PPh_3].[31] The molecular structure of one of the two crystallographically independent molecules of **3** is shown in Figure 3; selected bond lengths and angles are listed in Table 2. The cluster consists of a triangular Os_3 core with nine terminal carbonyl ligands. Three diphenyl(2-thienyl) ligands, each one coordinated to an osmium atom, occupy equatorial sites in such a way as to minimize steric interactions. The Os–Os distances average 2.894 Å, which is slightly longer than that found for $[Os_3(CO)_{12}]$ (vide supra), and the Os–P distances are comparable to those observed in compound **2**. It is worth noting that the introduction of the three diphenyl(2-thienyl)phosphane ligands results in a significant twisting of the $Os(CO)_3(Ph_2PC_4H_3S)$ units with respect to the Os_3 plane. This distortion towards D_3 symmetry, which presumably occurs to minimize the steric interaction of the large phosphane ligands and may be rationalised in terms of more effective ligand packing, has been observed previously for related mono-, di- and tri-substituted complexes.[29,31,32] The usual arrangement of the phosphane substituents, with one lying below the metal plane and the other two lying above, is found in both of the conformationally distinct molecules that are present in the asymmetric unit. However, these conformational isomers differ in the orientations of the phosphane substituents. In the isomer shown in Figure 3, the two substituents on the same side of the metal plane are one phenyl and one thienyl ring for all three phosphane ligands, and the sulfur atom points towards the inner part of the phosphane cone. In the other isomer, one phosphane ligand is rotated so that its thienyl group occupies the "other" side of the Os_3 plane.

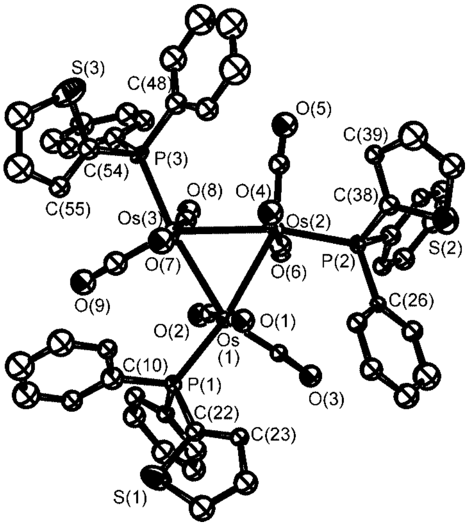

Figure 3. Molecular structure of one of the two crystallographically independent molecules of $[Os_3(CO)_9(Ph_2PC_4H_3S)_3]$ (**3**) (thermal ellipsoids at 30% probability). The carbon atoms of the carbonyl ligands bear the same numbering as the oxygen atoms. Hydrogen atoms have been omitted for clarity.

Table 2. Selected bond lengths [Å] and angles [°] for $[Os_3(CO)_9\{Ph_2P(C_4H_3S)\}_3]$ (**3**).

Molecule A			
Os(1)–Os(2)	2.902(1)	P(3)–C(42)	1.81(1)
Os(1)–Os(3)	2.877(2)	P(3)–C(48)	1.83(1)
Os(2)–Os(3)	2.904(1)	P(3)–C(54)	1.82(2)
Os(1)–P(1)	2.325(5)	Os(1)–C(1)	1.94(2)
Os(2)–P(2)	2.333(6)	Os(1)–C(2)	1.94(2)
Os(3)–P(3)	2.327(6)	Os(1)–C(3)	1.87(1)
P(1)–C(10)	1.82(1)	Os(2)–C(4)	1.86(2)
P(1)–C(16)	1.81(1)	Os(2)–C(5)	1.88(2)
P(1)–C(22)	1.83(2)	Os(2)–C(6)	1.89(3)
P(2)–C(26)	1.85(1)	Os(3)–C(7)	1.92(2)
P(2)–C(32)	1.82(1)	Os(3)–C(8)	1.86(2)
P(2)–C(38)	1.80(2)	Os(3)–C(9)	1.86(3)
C(1)–Os(1)–C(2)	172.0(9)	P(2)–Os(2)–Os(3)	165.7(1)
P(1)–Os(1)–C(3)	97.7(6)	C(5)–Os(2)–Os(1)	150.6(7)
P(1)–Os(1)–Os(2)	167.8(2)	C(5)–Os(2)–Os(3)	94.4(7)
P(1)–Os(1)–Os(3)	110.0(2)	C(7)–Os(3)–C(8)	170.1(9)
C(3)–Os(1)–Os(2)	93.0(6)	P(3)–Os(3)–Os(1)	171.2(2)
C(3)–Os(1)–Os(3)	151.4(6)	P(3)–Os(3)–Os(2)	111.9(1)
C(4)–Os(2)–C(6)	172.8(9)	C(9)–Os(3)–Os(1)	91.2(8)
P(2)–Os(2)–C(5)	99.0(7)	C(9)–Os(3)–Os(2)	149.9(8)
P(2)–Os(2)–Os(1)	108.6(1)		
Molecule B			
Os(4)–Os(5)	2.919(1)	P(6)–C(101)	1.83(1)
Os(4)–Os(6)	2.903(1)	P(6)–C(107)	1.83(1)
Os(5)–Os(6)	2.912(1)	P(6)–C(113)	1.78(3)
Os(4)–P(4)	2.347(5)	Os(4)–C(60)	1.85(3)
Os(5)–P(5)	2.331(6)	Os(4)–C(61)	1.90(2)
Os(6)–P(6)	2.342(6)	Os(4)–C(62)	1.90(2)
P(4)–C(69)	1.76(2)	Os(5)–C(63)	1.90(2)
P(4)–C(75)	1.88(1)	Os(5)–C(64)	1.90(2)
P(4)–C(81)	1.82(2)	Os(5)–C(65)	1.90(2)
P(5)–C(85)	1.81(1)	Os(6)–C(66)	1.87(1)
P(5)–C(91)	1.82(1)	Os(6)–C(67)	1.89(2)
P(5)–C(97)	1.82(2)	Os(6)–C(68)	1.89(2)
C(61)–Os(4)–C(62)	175.6(9)	P(5)–Os(5)–Os(6)	164.4(1)
P(4)–Os(4)–C(60)	96.7(7)	C(64)–Os(5)–Os(4)	163.8(7)
P(4)–Os(4)–Os(5)	161.7(1)	C(64)–Os(5)–Os(6)	106.6(7)
P(4)–Os(4)–Os(6)	102.4(1)	P(6)–Os(6)–C(66)	99.8(7)
C(60)–Os(4)–Os(5)	101.5(7)	P(6)–Os(6)–Os(4)	154.6(1)
C(60)–Os(4)–Os(6)	159.3(7)	P(6)–Os(6)–Os(5)	95.3(1)
C(63)–Os(5)–C(65)	172.1(9)	C(66)–Os(6)–Os(4)	104.8(7)
P(5)–Os(5)–C(64)	89.0(7)	C(66)–Os(6)–Os(5)	164.9(7)
P(5)–Os(5)–Os(4)	105.1(1)		

Room-Temperature Reaction of $[H_2Os_3(CO)_{10}]$ with $(Ph_2PC_4H_3S)$

A colour change from purple to yellow was observed immediately upon mixing 1 equiv. of diphenyl(2-thienyl)phosphane with $[H_2Os_3(CO)_{10}]$ in dichloromethane at room temperature. Comparison of the IR and NMR spectra of the product to the known $[H_2Os_3(CO)_{10}(L)]$ clusters,[32] indicated that the product is $[HOs_3(\mu\text{-}H)(CO)_{10}\text{-}\{Ph_2P(C_4H_3S)\}]$ (**4**), which was isolated in 26% yield after TLC purification. The room-temperature ^1H NMR spectrum shows a broad hydrido signal ($\delta \approx -15$ ppm) due to rapid exchange of the two hydrido ligands, but at –35 °C the exchange is frozen out and two distinct resonances are observed in the hydrido region – one for the terminal hydrido ligand at $\delta = -10.2$ ppm and one for the bridging hydrido ligand at $\delta = -19.7$ ppm. The $^{31}P\{^1H\}$ NMR spectrum displays one singlet at $\delta = -16.7$ ppm. On the basis of these NMR spectra we propose that the phosphane ligand in **4** is situated *trans* to the Os–Os bond and *cis* to the bridging hydrido ligand, which is reported as the thermodynamically most favourable of the isomers of $[HOs_3(\mu\text{-}H)(CO)_{10}(\text{phosphane})]$ that have been identified.[33,34] Earlier investigations have shown that four more isomers have been detected from the reaction between $[H_2Os_3(CO)_{10}]$ and phosphanes.[35] In contrast to those results, we did not observe any additional isomers, even at –75 °C. This lack of observation of isomers may be related to the relative bulk of the ligand, making the other possible isomers sterically unfavourable. An alternative explanation is that the populations of (transient) isomers were too low to be observed.

Thermal Treatment of $[H_2Os_3(CO)_{10}]$ with $Ph_2P(C_4H_3S)$

Reaction of an excess of diphenyl(2-thienyl)phosphane with $[H_2Os_3(CO)_{10}]$ in refluxing toluene for 3 h gives a colour change from initial purple colour to yellow, then to dark green and ultimately to brown. Separation by TLC led to the isolation of three products.

The first product was isolated in 21% yield. Although IR spectra of isostructural Os and Ru clusters are not always comparable, the product was identified as the cyclometallated cluster $[(\mu\text{-}H)Os_3(CO)_9\{\mu_3\text{-}Ph_2P(C_4H_2S)\}]$ (**5**) on the basis of the similarity of its IR spectrum to that of the known cluster $[Ru_3(\mu\text{-}H)(CO)_9\{\mu_3\text{-}Ph_2P(C_4H_2S)\}]$.[20] Mass spectrometric and microanalytical data were found to be consistent with the proposed formula. The ^1H NMR spectrum displays a doublet at $\delta = -18.0$ ppm confirming the presence of a bridging hydrido ligand, which couples to one phosphorus atom ($J_{P\text{–}H} = 13.2$ Hz). In the phenyl region, two *ortho* signals are observed, corresponding to two isomers. This is similar to that previously observed for $[Ru_3(\mu\text{-}H)(CO)_9\{\mu_3\text{-}Ph_2P(C_4H_2S)\}]$.[20] Unlike the ruthenium analogue, where the *ortho*-protons are fluxional at 20 °C and only become static on the NMR timescale at –20 °C, the *ortho*-protons of **5** were not fluxional at ambient temperature. The $^{31}P\{^1H\}$ NMR spectrum of **5** at 27 °C displays a singlet at $\delta = -3.3$ ($^1J_{P\text{–}Os} = 147$ Hz) ppm, with a small change of shift to $\delta = -5.3$ ppm at –80 °C. The small $^1J_{P\text{–}Os}$ coupling of 147 Hz is in agreement with axial coordination of the phosphorus atom with respect to the plane of the metal triangle. Typical equatorial $^1J_{P\text{–}Os}$ couplings are of the order of 185–225 Hz while axial couplings are much smaller as the metal–phosphane bond is no longer aligned with the electron density of the metal triangle.[36–39]

It was possible to grow crystals suitable for X-ray diffraction for cluster **5**, and single-crystal diffraction studies were undertaken in order to confirm the structure. The molecular structure of **5** is shown in Figure 4; selected bond lengths and angles are listed in Table 3. $[Os_3(\mu\text{-}H)(CO)_9\{\mu_3\text{-}Ph_2P(C_4H_2S)\}]$ (**5**) crystallises with two independent slightly different conformers in the asymmetric unit and is isostructural with $[(\mu\text{-}H)Ru_3(CO)_9\{\mu_3\text{-}Ph_2P(C_4H_2S)\}]$.[20] Compound **5** consists of an irregular triangle of osmium atoms, each of which is coordinated by three carbonyl ligands. A triply bridging diphenyl(2-thienyl)phosphane ligand and a bridging hydrido ligand complete the coordination sphere of the cluster. The $\mu_3\text{-}Ph_2P(C_4H_2S)$ ligand, which acts as a five-electron donor, is coordinated through the phosphorus atom in axial position to Os(1) and through the *ortho*-metallated thienyl ring to Os(3) with a C(11)–Os(3) σ-bond [Os(3)–C(11) 2.10(1) and 2.09(1) Å in molecule A and B] and to Os(2) with an $\eta^2(\pi)$-interaction between C(10)–C(11) and Os(2) [Os(2)–C(10) 2.34(1) and 2.36(1) Å, Os(2)–C(11) 2.35(1) and 2.32(1) Å in A and B, respectively]. This σ,η^2-vinyl-type interaction is not unprecedented; it has, for example, been observed in $[(\mu\text{-}H)Ru_3(CO)_9\{\mu_3\text{-}Ph_2P(C_4H_2S)\}]$[20] and $[(\mu\text{-}H)Ru_3(CO)_9\{\mu_3\text{-}Ph_2P(C_8H_4S)\}]$ (C_8H_4S = benzothienyl),[40] $[Os_3(\mu\text{-}H)(CO)_9(\mu\text{-}Ph_2PCH{=}CH)]$,[34] $[Os_3(\mu\text{-}H)(CO)_9\{\mu_3\text{-}PMePh(C_6H_4)\}]$[41] as well as in the closely related $[Os_3(\mu\text{-}H)(MeSC_4H_2S)(CO)_9]$,[42] in which the Ph_2P unit in **5** is substituted by an SMe group. The C_4H_2S ring is tilted with respect to the Os_3 plane [dihedral angle between the Os_3 and C_4H_2S planes 129.2(3) and 128.5(5)° for A and B, respectively] as has previously been noticed for the triruthenium analogue $[(\mu\text{-}H)Ru_3(CO)_9\{\mu_3\text{-}Ph_2P(C_4H_2S)\}]$[20] and $[Os_3(\mu\text{-}H)(MeSC_4H_2S)(CO)_9]$.[42] This tilt of the thienyl ring, which has been found also for the *ortho*-metallated phenyl ring in $[Os_3(\mu\text{-}H)(CO)_9\{\mu_3\text{-}PMePh(C_6H_4)\}]$,[41] takes place in order

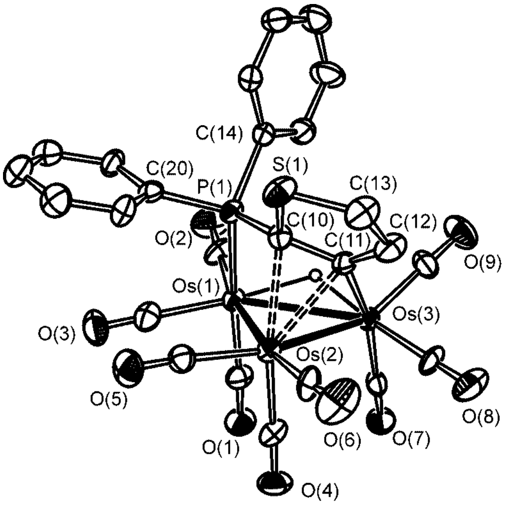

Figure 4. Molecular structure of one of the two crystallographically independent molecules of $[(\mu\text{-}H)Os_3(CO)_9\{\mu_3\text{-}Ph_2P(C_4H_2S)\}]$ (**5**) (thermal ellipsoids at 30% probability). The carbon atoms of the carbonyl ligands bear the same numbering as the oxygen atoms. All hydrogen atoms except the hydrido ligand have been omitted for clarity.

Table 3. Selected bond lengths [Å] and angles [°] for [(μ-H)$Os_3(CO)_9\{\mu_3\text{-}Ph_2P(C_4H_2S)\}$] (**5**). The values in brackets refer to molecule B.

Os(1A)–Os(2A)	2.857(1) [2.859(1)]	S(1A)–C(13A)	1.70(1) [1.72(1)]
Os(1A)–Os(3A)	3.004(1) [3.020(1)]	C(12A)–C(13A)	1.89(1) [1.89(2)]
Os(2A)–Os(3A)	2.755(1) [2.762(1)]	S(1A)–C(13A)	1.70(1) [1.72(1)]
Os(1A)–H(1A)	1.84(2) [1.83(2)]	C(12A)–C(13A)	1.34(2) [1.32(2)]
Os(3A)–H(1A)	1.82(2) [1.83(2)]	Os(1A)–C(3A)	1.90(2) [1.90(1)]
Os(1A)–P(1A)	2.350(3) [2.344(3)]	Os(2A)–C(4A)	1.88(1) [1.85(1)]
Os(2A)–C(11A)	2.35(1) [2.32(1)]	Os(2A)–C(4A)	1.88(1) [1.85(1)]
Os(3A)–C(11A)	2.35(1) [2.32(1)]	Os(2A)–C(4A)	1.88(1) [1.85(1)]
P(1A)–C(10A)	2.10(1) [2.09(1)]	Os(2A)–C(6A)	1.88(1) [1.90(2)]
P(1A)–C(14A)	1.77(1) [1.78(1)]	Os(3A)–C(7A)	1.93(1) [1.93(1)]
P(1A)–C(20A)	1.832(7) [1.831(6)]	Os(3A)–C(8A)	1.89(1) [1.88(1)]
C(10A)–C(11A)	1.801(6) [1.827(7)]	Os(3A)–C(9A)	1.89(1) [1.88(1)]
Os(1A)–C(1A)	1.45(1) [1.43(1)]	C(10A)–S(1A)	1.77(1) [1.78(1)]
Os(1A)–C(2A)	1.93(1) [1.93(1)]	C(11A)–C(12A)	1.46(2) [1.45(2)]
C(2A)–Os(1A)–C(3A)	95.6(6) [95.7(7)]	C(5A)–Os(2A)–Os(3A)	160.4(4) [160.9(4)]
P(1A)–Os(1A)–C(1A)	170.3(4) [168.5(5)]	C(6A)–Os(2A)–Os(1A)	170.1(4) [169.4(4)]
P(1A)–Os(1A)–Os(2A)	73.90(7) [74.53(8)]	C(6A)–Os(2A)–Os(3A)	105.4(4) [105.0(4)]
P(1A)–Os(1A)–Os(3A)	86.17(7) [86.03(7)]	C(11A)–Os(2A)–Os(3A)	47.7(3) [47.5(3)]
C(2A)–Os(1A)–Os(2A)	167.7(4) [168.5(4)]	C(7A)–Os(3A)–C(11A)	165.6(5) [166.0(5)]
C(2A)–Os(1A)–Os(3A)	119.1(5) [116.4(4)]	C(8A)–Os(3A)–C(9A)	95.5(7) [94.0(6)]
C(3A)–Os(1A)–Os(2A)	90.0(4) [92.5(5)]	C(8A)–Os(3A)–Os(2A)	92.7(5) [95.5(5)]
C(3A)–Os(1A)–Os(3A)	145.4(4) [147.9(5)]	C(8A)–Os(3A)–Os(1A)	150.3(5) [152.3(5)]
C(5A)–Os(2A)–C(6A)	94.1(5) [93.9(6)]	C(9A)–Os(3A)–Os(2A)	155.3(4) [151.4(4)]
C(5A)–Os(2A)–Os(1A)	95.8(4) [96.0(4)]	C(9A)–Os(3A)–Os(1A)	114.1(5) [113.5(4)]

to favour the η²-interaction. The hydrido ligand which, as expected, is bridging the longest edge of the cluster, was located directly in the electron-density map. In both molecules, the hydrido ligand is on the same side of the Os_3 plane as the μ_3-$Ph_2P(C_4H_2S)$ ligand [ca. 0.4 Å above the metal plane]. The Os–P bond lengths [Os(3)–P(1) 2.350(3) and 2.344(3) Å in A and B, respectively] are similar to those found in the cyclometallated compounds [$Os_3(\mu\text{-}H)(CO)_9\{\mu\text{-}Ph_2P(CH{=}CH)\}$][34] [2.361(4) Å] and [$Os_3(\mu\text{-}H)(CO)_9\{\mu_3\text{-}PMePh(C_6H_4)\}$][41] [2.342(6) Å].

The second product, which was isolated in 34% yield, was identified as [(μ-H)$Os_3(CO)_8\{\mu_3\text{-}Ph_2P(C_4H_2S)\}\{Ph_2P(C_4H_3S)\}$] (**6**). The IR spectrum of **6** is similar to that of [(μ-H)$Ru_3(CO)_8\{\mu_3\text{-}Ph_2P(C_8H_4S)\}\{Ph_2P(C_8H_5S)\}$][40] and mass spectrometric and microanalytical data are consistent with the proposed formula. The variable-temperature ^1H and $^{31}P\{^1H\}$ NMR spectra of **6** demonstrate that this complex is highly fluxional. The $^{31}P\{^1H\}$ NMR spectrum of **6** at 20 °C shows two doublets at δ = –0.63 and –1.48 (J_{P-P} = 16.6 Hz) ppm (Figure 5). This is supported by the bridging hydrido signal (δ = –17.4 ppm), appearing as a doublet of doublets due to the coupling to two non-equivalent phosphorus ligands. At –100 °C, the spectrum freezes out to show two distinct isomers in both the $^{31}P\{^1H\}$ and ^1H NMR spectra, although the ^1H spectrum had to be acquired at 600 MHz before the shift differences could be clearly discerned (Figure 5). The limiting $^{31}P\{^1H\}$ spectrum (–100 °C) shows two pairs of doublets centred at $\delta \approx$ 1.2 ppm, while the signal in the hydrido region of the ^1H spectrum is shifted upfield and split into two doublets of doublets. It is possible that the two isomers that are observed in solution are related by the relative location of the terminal phosphane ligand with respect to the hydrido ligand. This is supported by the observed differences in the phosphane–hydrido couplings. We believe that this may be explained in terms of an oscillation of the thienyl group identical to that observed for **5** (vide supra) except that, unlike **5**, the isomers of **6** (Figure 6) are observable by NMR due to the presence of the terminally coordinated phosphane ligand, which renders the two hydrido positions non-equivalent.

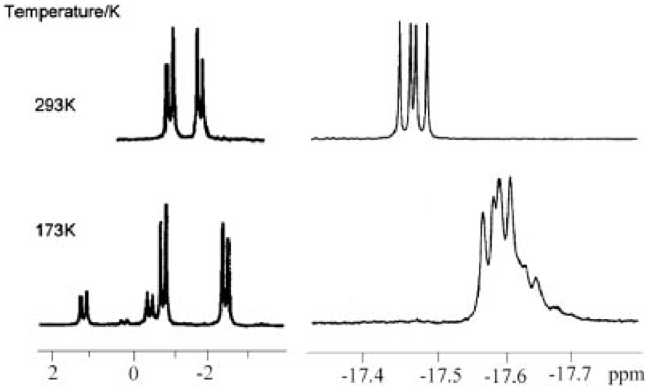

Figure 5. $^{31}P\{^1H\}$ and ^1H NMR spectra of [(μ-H)$Os_3(CO)_8\{\mu_3\text{-}Ph_2P(C_4H_2S)\}\{Ph_2P(C_4H_3S)\}$] (**6**) at 293 K and 173 K. The low-temperature ^1H NMR spectrum (CD_2Cl_2, 600 MHz) shows the very small shift differences between the two isomers.

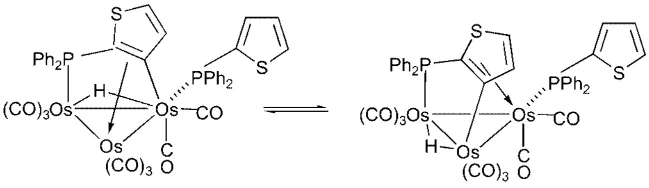

Figure 6. Proposed structures of the two isomers of **6**.

The assignment of the room-temperature structure could be confirmed by the acquisition of a ^{187}Os NMR spectrum by inverse methods.[38] The presence of a P–P coupling makes it potentially more difficult to extract the $^{1}J_{Os-P}$ values directly from a $^{31}P\{^{1}H\}$ spectrum. The ^{1}H-^{187}Os 2D HMQC spectrum at –100 °C (Figure 7) shows two shifts (δ = –13965 and –13230 ppm), corresponding to two osmium centres directly bonded to the bridging hydrido ligands, and it is possible to extract the two $^{1}J_{Os-P}$ couplings of 147 Hz and 211 Hz from the HMQC spectrum. The first coupling constant corresponds to that observed for **5** (147 Hz) and the coupling constant of 211 Hz is similar to other known $^{1}J_{Os-P}$ values for terminal phosphane ligands.[39] The fact that the $^{1}J_{Os-P}$ values for the axial phosphane ligands in **5** and **6** are identical is surprising (and may be coincidental), but it is indicative of the low level of electronic communication between the metal centres in the clusters.

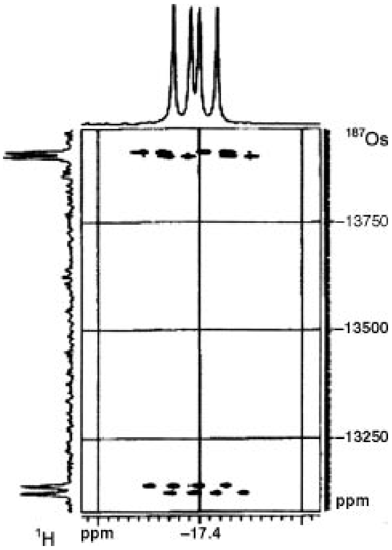

Figure 7. 2D ^{1}H-^{187}Os HMQC spectrum of **6** which clearly demonstrates the two different ^{187}Os-^{31}P couplings for each of the hydrido-bridged osmium centres (cf. Figure 5).

It was possible to grow crystals suitable for X-ray diffraction for cluster **6**, and a single-crystal diffraction study was undertaken in order to confirm its structure and investigate whether isomers could be detected also in the solid state. The structure of $[Os_3(\mu\text{-}H)(CO)_8\{\mu_3\text{-}Ph_2P(C_4H_2S)\}\{Ph_2P(C_4H_3S)\}]$ (**6**) is shown in Figure 8; selected bond lengths and angles are listed in Table 4.

As expected, the structure is similar to that of $[(\mu\text{-}H)Ru_3(CO)_8\{\mu_3\text{-}Ph_2P(C_4H_2S)\}\{Ph_2P(C_4H_3S)\}]$[20] and of $[(\mu\text{-}H)Ru_3(CO)_8\{\mu_3\text{-}Ph_2P(C_8H_4S)\}\{Ph_2P(C_8H_5S)\}]$.[40] It is also closely related to $[Ru_3(\mu\text{-}H)(CO)_8\{\mu_3\text{-}Ph_2P(CH{=}CH)\}\{Ph_2P(CH{=}CH_2)\}]$[43] and differs from **5** only in the substitution of one carbonyl ligand by one terminal thienylphosphane ligand. The cluster consists of a scalene triangle of Os atoms [Os(1)–Os(2) 3.014, Os(1)–Os(3) 2.863 Å, Os(2)–Os(3) 2.780(1) Å] bound to eight terminal carbonyl ligands, a terminal $Ph_2PC_4H_3S$ ligand, a μ_3-$Ph_2PC_4H_2S$ and a μ_2-bridging hydrido ligand. The μ_3-$Ph_2PC_4H_2S$ ligand behaves as a five-electron donor and interacts with all three metal atoms in the same fashion as observed in **5**. The σ- and η^2-interactions of the *ortho*-metallated thienyl ring [Os(2)–C(22) 2.10(1), Os(3)–C(21) 2.32(1) and Os(3)–C(22) 2.33(1) Å] are very similar to those found in **5** and unaffected by the presence of the terminal phosphane ligand. The C(21)–C(22) distance [1.45(1) Å] in the bridging thienyl ring is identical to the equivalent interaction in **5** and similar to the analogous bonds in $[(\mu\text{-}H)Ru_3(CO)_8\{\mu_3\text{-}Ph_2P(C_4H_2S)\}\{Ph_2P(C_4H_3S)\}]$[20] [1.425(5) Å]. The terminal diphenyl(2-thienyl)phosphane ligand is coordinated in an equatorial position, but the phosphorus atom is displaced out of the metal plane [P(2) +1.034(2) Å] on the same side of the μ_3-$Ph_2PC_4H_2S$ ligand. The two Os–P interactions [Os(1)–P(1)

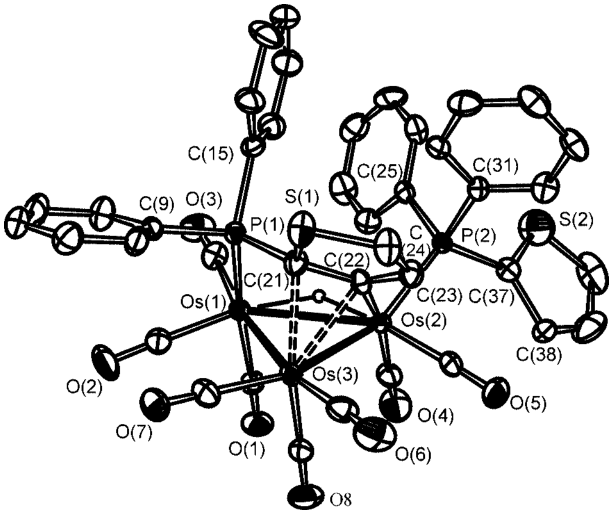

Figure 8. Molecular structure of $[(\mu\text{-}H)Os_3(CO)_8\{\mu_3\text{-}Ph_2P(C_4H_2S)\}\{Ph_2P(C_4H_3S)\}]$ (**6**) (thermal ellipsoids at 30% probability). The carbon atoms of the carbonyl ligands bear the same numbering as the oxygen atoms. All hydrogen atoms except the hydrido ligand have been omitted for clarity.

Table 4. Selected bond lengths [Å] and angles [°] for $[(\mu\text{-}H)Os_3(CO)_8\{\mu_3\text{-}Ph_2P(C_4H_2S)\}\{Ph_2P(C_4H_3S)\}]$ (**6**).

Os(1)–Os(2)	3.0142(6)	P(2)–C(37)	1.805(9)
Os(1)–Os(3)	2.8626(7)	C(21)–C(22)	1.45(1)
Os(2)–Os(3)	2.7799(8)	C(21)–S(1)	1.77(1)
Os(1)–H(1)	1.84(3)	C(23)–C(24)	1.35(1)
Os(2)–H(1)	1.85(3)	Os(1)–C(1)	1.93(1)
Os(1)–P(1)	2.360(2)	Os(1)–C(2)	1.86(1)
Os(2)–P(2)	2.325(3)	Os(1)–C(3)	1.93(1)
Os(2)–C(22)	2.10(1)	Os(2)–C(4)	1.92(1)
Os(3)–C(21)	2.32(1)	Os(2)–C(5)	1.83(1)
Os(3)–C(22)	2.33(1)	Os(3)–C(6)	1.90(1)
P(1)–C(9)	1.835(5)	Os(3)–C(7)	1.91(1)
P(1)–C(15)	1.839(6)	Os(3)–C(8)	1.86(1)
P(1)–C(21)	1.793(9)	C(22)–C(23)	1.46(1)
P(2)–C(25)	1.833(5)	S(1)–C(24)	1.69(1)
P(2)–C(31)	1.811(5)		
C(2)–Os(1)–C(3)	96.4(5)	P(2)–Os(2)–C(22)	99.9(3)
P(1)–Os(1)–C(2)	92.3(3)	P(2)–Os(2)–Os(1)	115.53(6)
P(1)–Os(1)–C(3)	98.2(3)	P(2)–Os(2)–Os(3)	153.52(6)
P(1)–Os(1)–Os(2)	87.37(6)	C(5)–Os(2)–Os(1)	151.0(3)
P(1)–Os(1)–Os(3)	72.88(6)	C(5)–Os(2)–Os(3)	93.9(3)
C(2)–Os(1)–Os(2)	145.1(4)	C(6)–Os(3)–C(7)	93.6(6)
C(2)–Os(1)–Os(3)	90.2(4)	C(7)–Os(3)–C(8)	99.3(5)
C(3)–Os(1)–Os(2)	118.2(3)	C(6)–Os(3)–Os(1)	169.2(3)
C(3)–Os(1)–Os(3)	169.1(3)	C(6)–Os(3)–Os(2)	105.6(4)
P(2)–Os(2)–C(4)	93.2(4)	C(7)–Os(3)–Os(1)	95.9(4)
P(2)–Os(2)–C(5)	93.3(4)	C(7)–Os(3)–Os(2)	160.2(4)

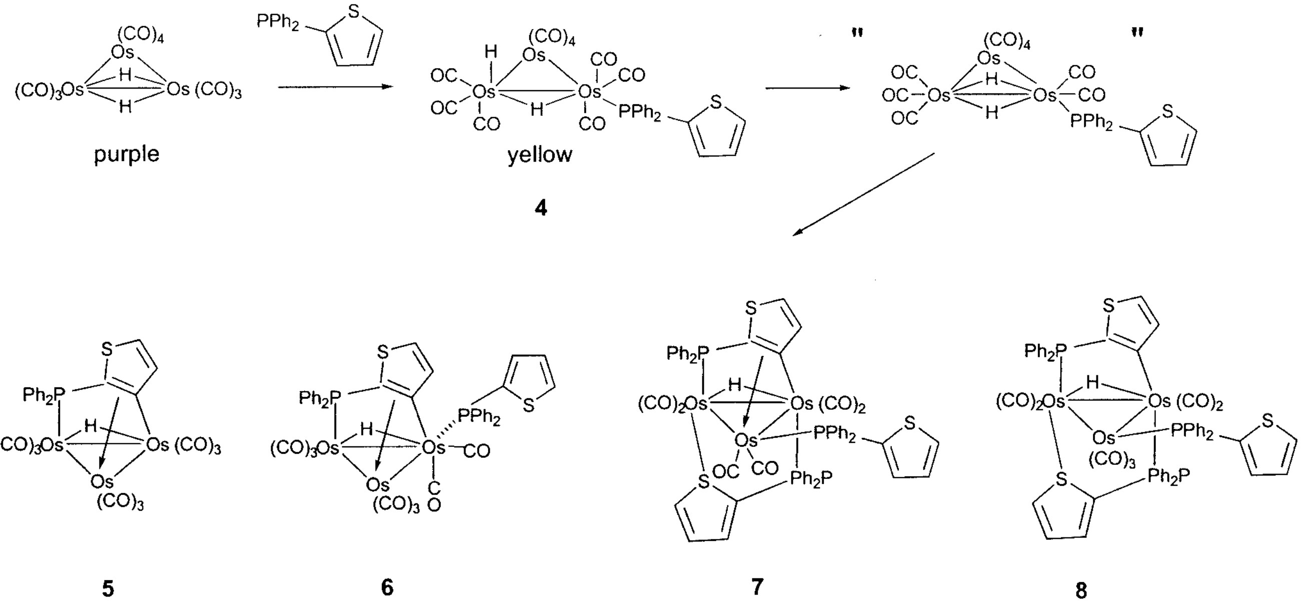

Scheme 3. Possible reaction scheme for the reaction between $[H_2Os_3(CO)_{10}]$ and $Ph_2P(C_4H_3S)$ in toluene.

2.360(2) and Os(2)–P(2) 2.325(3) Å] are not equivalent; the Os–P(axial) distance is longer than the Os–P(equatorial) but very similar to the corresponding distance in **5**. The bridging hydrido ligand has been directly located along the Os(1)–Os(2) edge which is, as usual, the longest Os–Os interaction.

The third product, compound **7**, was isolated in 5% yield. The mass spectrometric analysis suggests the stoichiometric formula $[Os_3(CO)_6\{Ph_2P(C_4H_3S)\}_3]$ for this product, and microanalytical data are consistent with the proposed formula. The ^1H NMR spectrum displays a signal in the (bridging) hydrido region (δ = –16.67 ppm) indicating that an *ortho*-metallation has taken place. The hydrido signal appears as a triplet (overlapping doublet of doublets), indicating coupling to two non-equivalent phosphorus atoms. Three signals are observed in the $^{31}P\{^1H\}$ NMR spectrum, confirming the presence of three non-equivalent phosphorus atoms; a multiplet at δ = 4.50 ppm, a doublet at δ = –1.65 (J_{P-P} = 16 Hz) ppm and a multiplet at δ = –5.98 ppm. On the basis of these data, we propose the molecular formula $[(\mu\text{-}H)Os_3(CO)_6\{\mu_3\text{-}Ph_2P(C_4H_2S)\}\{\mu_2\text{-}Ph_2P(C_4H_3S)\}\{Ph_2P(C_4H_3S)\}]$ (cf. Scheme 3) for compound **7**, containing three diphenyl(2-thienyl) ligands coordinated in three different coordination modes; a μ_3-fashion, a μ-(P,S) fashion and a terminal fashion. The μ-(P,S) coordination mode has been detected for a diphenyl(2-benzothienyl)phosphane derivative of $[Os_3(CO)_{12}]$[44] as well as in thienylphosphane derivatives of $[Rh_6(CO)_{16}]$.[45]

The fourth product, compound **8**, was isolated in 3% yield. The mass spectrum of this compound indicates that it has one more carbonyl ligand than compound **7**. The ^1H NMR spectrum displays, in addition to signals of aromatic hydrogen atoms, a triplet (overlapping doublet of doublets) at δ = –17.05 ppm, thus confirming the presence of a single bridging hydrido ligand. In the $^{31}P\{^1H\}$ NMR spectrum, three non-equivalent phosphorus resonances are observed at δ = –3.19 (m), –5.30 (d) and –9.15 (m) ppm. These data suggest that this complex and compound **7** are structurally similar except for one carbonyl ligand. Therefore, we propose the molecular formula $[(\mu\text{-}H)Os_3(CO)_7\{\mu\text{-}Ph_2P(C_4H_2S)\}\{\mu\text{-}Ph_2P(C_4H_3S)\}\{Ph_2P(C_4H_3S)\}]$ for compound **8**, containing the $\mu\text{-}Ph_2P(C_4H_2S)$ ligand bonded through P and a σ-interaction to the osmium triangle, but lacking an η^2-interaction with an osmium atom (cf. Scheme 3).

Several colour changes were observed during the reaction of diphenyl(2-thienyl)phosphane with $[H_2Os_3(CO)_{10}]$, indicating that the reaction proceeds via a number of intermediates. A possible reaction scheme is shown in Scheme 3. Addition of the ligand to the cluster results in an immediate colour change from purple to yellow and formation of $[HOs_3(\mu\text{-}H)(CO)_{10}\{Ph_2P(C_4H_3S)\}]$ (**4**) (indicated by IR spectroscopy). Cluster **4** then reacts further, possibly undergoing a loss of one CO ligand and forming an unsaturated intermediate cluster which is likely to be $[H_2Os_3(CO)_9\{Ph_2P(C_4H_3S)\}]$. It has previously been observed, that heating solutions of compounds of the type $[H_2Os_3(CO)_{10}(L)]$ (L = tertiary phosphane), leads to a loss of one carbonyl ligand giving $[H_2Os_3(CO)_9(L)]$.[33,46] $[H_2Os_3(CO)_9\{Ph_2P(C_4H_3S)\}]$ then presumably undergoes further decarbonylation ultimately giving rise to the four products isolated.

Conclusion

In conclusion, the introduction of diphenyl(2-thienyl)phosphane into the coordination sphere of triosmium clusters by direct thermal substitution of carbonyl ligands or room-temperature reaction with the unsaturated cluster $[H_2Os_3(CO)_{10}]$ is facile. In all cases surveyed in this study, the ligand initially coordinates as a monodentate phosphane, but further activation/metallation of the ligand is possible at elevated temperatures, although the osmium clusters are considerably less reactive than their ruthenium analogues.[20]

Experimental Section

General Remarks: The clusters [$Os_3(CO)_{12}$][47] and [$Os_3(\mu\text{-}H)_2(CO)_{10}$][48–50] and the ligand diphenyl(2-thienyl)phosphane[20] were synthesised by published methods. Solvents were dried by standard methods prior to use. TLC was performed on commercial plates precoated with Merck Kieselgel 60 to 0.5 mm thickness. NMR spectra were acquired with Bruker DRX300 WB, DRX500 and DRX600 spectrometers. Gradient-selected ^{187}Os 2D HMQC experiments were carried out with a Bruker DMX600 equipped with an XYZ 10A gradient amplifier (*z*-gradient strength 0.05 T m^{-1}). Details regarding the experimental setup and acquisition parameters for the ^{187}Os 2D HMQC experiments are listed in the Supporting Information (see footnote on the first page of this article). IR spectra were acquired with a Nicolet Avatar FT-IR spectrometer and FAB-MS (3-nitrobenzyl alcohol matrix) data with a JEOL SX-102 mass spectrometer.

Direct Thermal Reaction of [$Os_3(CO)_{12}$] and Diphenyl(2-thienyl)phosphane in Toluene: A solution of [$Os_3(CO)_{12}$] (300 mg, 0.33 mmol) and diphenyl(2-thienyl)phosphane (98 mg, 0.37 mmol) in toluene (40 mL) was refluxed under nitrogen for 2.5 h. The solvent was removed under reduced pressure. Preparative TLC of the residue, using dichloromethane/*n*-hexane (3:7, v/v) as eluent gave four compounds, in order of decreasing R_f: [$Os_3(CO)_{12}$] (pale yellow, trace), [$Os_3(CO)_{11}\{Ph_2P(C_4H_3S)\}$] (**1**, intense yellow, 96 mg, 23%), [$Os_3(CO)_{10}\{Ph_2P(C_4H_3S)\}_2$] (**2**, intense yellow, 203 mg, 44%), [$Os_3(CO)_9\{Ph_2P(C_4H_3S)\}_3$] (**3**, orange, 42 mg, 8%).

1: $C_{27}H_{13}O_{11}Os_3PS$ (1147.12): calcd. C 28.27, H 1.14, P 2.76; found C 28.19, H 1.33, P 2.76. FAB-MS: *m/z* = 1148 [M$^+$], [M$^+$ – *n* CO, *n* = 1–11]. IR (CH_2Cl_2): $\tilde{\nu}_{co}$ = 2108 s, 2056 s, 2031 sh, 2018 sh, 1988 m, 1958 sh cm^{-1}. ^{1}H NMR (300 MHz, $CDCl_3$, 30 °C): δ = 7.9–7.1 (m, 13 H, arom.) ppm. ^{31}P NMR (300 MHz, $CDCl_3$, 30 °C): δ = –16.2 (s, 1 P, terminal phosphane) ppm.

2: $C_{42}H_{26}O_{10}Os_3P_2S_2$ (1387.42): calcd. C 36.36, H 1.89, P 4.46; found C 36.33, H 1.62, P 4.94. FAB-MS: *m/z* = 1388 [M$^+$], [M$^+$ – *n* CO, *n* = 1–10]. IR (CH_2Cl_2): $\tilde{\nu}_{co}$ = 2086 w, 2070 s, 2031 s, 1999 s, 1970 w, 1956 w cm^{-1}. ^{1}H NMR (300 MHz, $CDCl_3$, 20 °C): δ = 7.82–7.17 (m, 26 H, arom.) ppm. ^{31}P NMR (300 MHz, CD_2Cl_2, –60 °C): δ = –18.12 (s, 1 P, terminal), –18.26 (s, 2 P, terminal), –21.97 (s, 1 P, terminal) ppm.

3: $C_{57}H_{39}O_9Os_3P_3S_3$ (1627.72): calcd. C 42.06, H 2.42, P 5.71: found C 42.48, H 2.85, P 5.23. FAB-MS: *m/z* = 1628 [M$^+$], 1600 [M$^+$ – CO]. IR (CH_2Cl_2): $\tilde{\nu}_{co}$ = 2068 sh, 2034 sh, 2013 w, 1998 m, 1975 m, 1945 w cm^{-1}. ^{1}H NMR (500 MHz, $CDCl_3$, 25 °C): δ = 7.6–7.12 (m, 39 H, arom.) ppm. ^{31}P NMR (500 MHz, $CDCl_3$, 25 °C): δ = –17.2 (s, 3 P, terminal) ppm.

Room-Temperature Reaction of [$H_2Os_3(CO)_{10}$] with Diphenyl(2-thienyl)phosphane in CH_2Cl_2: Diphenyl(2-thienyl)phosphane (2 equiv., 95 mg, 0.36 mmol) was added to [$H_2Os_3(CO)_{10}$] (1 equiv., 150 mg, 0.18 mmol) in freshly distilled dichloromethane (30 mL) at room temperature under nitrogen. Within 5 min, the solution turned from purple to yellow and the IR spectrum indicated that no starting material had remained unreacted. The solution was concentrated and absorbed onto TLC plates using dichloromethane/*n*-hexane (3:7, v/v) as eluent. Two bands were recovered, in order of decreasing R_f: [$HOs_3(\mu\text{-}H)(CO)_{10}\{Ph_2P(C_4H_3S)\}$] (**4**, 34 mg, 26%, yellow), uncharacterised product (5 mg, 4%, red).

4: $C_{26}H_{15}O_{10}Os_3PS$ (1121.12): calcd. C 27.85, H 1.35, P 2.76; found C 28.86, H 1.38, P 2.72. FAB-MS: *m/z* = 1120 [M$^+$], [M$^+$ – *n* CO, *n* = 1–10]. IR (CH_2Cl_2): $\tilde{\nu}_{co}$ = 2106 s, 2090 m, 2086 m, 2068 s, 2052 s, 2025 s, 1984 m, 1972 m, 1933 sh cm^{-1}. ^{1}H NMR (300 MHz, $CDCl_3$, 20 °C): δ = 7.79–7.27 (m, 13 H, arom.), –10 to –20 (br. s, 2 H, hydrido) ppm. ^{1}H NMR (300 MHz, $CDCl_3$, –45 °C): δ = 7.8–7.3 (m, 13 H, arom.), –10.12 (d, $J_{H,H}$ = 3.3 Hz, 1 H, terminal hydrido), –19.72 (dd, $J_{H,H}$ = 3.3 Hz, $J_{P,H}$ = 11 Hz, 1 H, bridging hydrido) ppm. ^{31}P NMR (300 MHz, $CDCl_3$, –45 °C): δ = –16.7 (s, 1 P, terminal phosphane) ppm.

Thermal Reaction of [$H_2Os_3(CO)_{10}$] with Diphenyl(2-thienyl)phosphane in Toluene: A solution of [$H_2Os_3(CO)_{10}$] (150 mg, 0.18 mmol) and ($Ph_2PC_4H_3S$) (95 mg, 0.36 mmol) in toluene (30 mL) was refluxed under nitrogen for 3 h. During the reaction the colour changed from purple to yellow, to green, and finally to brown. The products were separated by TLC using dichloromethane/*n*-hexane (2:3, v/v) as eluent. Five bands were recovered, in order of decreasing R_f: [$H_2Os_3(CO)_{10}$] (purple, trace), [$(\mu\text{-}H)Os_3(CO)_9\{\mu_3\text{-}Ph_2P(C_4H_2S)\}$] (**5**, intense yellow, 99 mg, 21%), [$(\mu\text{-}H)Os_3(CO)_8\{\mu_3\text{-}Ph_2P(C_4H_2S)\}\{Ph_2P(C_4H_3S)\}$] (**6**, intense yellow, 197 mg, 34%), [$(\mu\text{-}H)Os_3(CO)_6\{\mu_3\text{-}Ph_2P(C_4H_2S)\}\{\mu\text{-}Ph_2P(C_4H_3S)\}\{Ph_2P(C_4H_3S)\}$] (**7**, yellow, 32 mg, 5%), [$(\mu\text{-}H)Os_3(CO)_7\{\mu\text{-}Ph_2P(C_4H_2S)\}\{\mu\text{-}Ph_2P(C_4H_3S)\}\{Ph_2P(C_4H_3S)\}$] (**8**, intense yellow, 22 mg, 3%).

5: $C_{25}H_{13}O_9Os_3PS$ (1091.1). FAB-MS: *m/z* = 1092 [M$^+$], [M$^+$ – *n* CO, *n* = 1–9]. IR (CH_2Cl_2): $\tilde{\nu}_{co}$ = 2088 s, 2060 s, 2034 s, 2019 s, 1989 s, 1974 w, 1965 m cm^{-1}. ^{1}H NMR (300 MHz, $CDCl_3$, 20 °C): δ = 7.93–7.07 (m, 12 H, arom.), –18.0 (d, $J_{H,P}$ = 13.2 Hz, 1 H, bridging hydrido) ppm. ^{31}P NMR (300 MHz, $CDCl_3$, 20 °C): δ = –3.27 (s, $J_{Os,P}$ = 147 Hz, 1 P, axial phosphorus) ppm.

6: $C_{40}H_{26}O_8Os_3P_2S_2$ (1331.4): calcd. C 36.09, H 1.97, P 4.65; found C 36.09, H 1.97, P 4.56. FAB-MS: *m/z* = 1332 [M$^+$], [M$^+$ – *n* CO, *n* = 1–8]. IR (CH_2Cl_2): $\tilde{\nu}_{co}$ = 2074 s, 2032 s, 2015 s, 1993 sh, 1981 m, 1967 m, 1957 m, 1945 sh cm^{-1}. ^{1}H NMR (300 MHz, $CDCl_3$, 20 °C): δ = 7.86–6.35 (m, 25 H, arom.), –17.4 (dd, $J_{H,P}$ = 15.4 Hz, $J_{H,P}$ = 11 Hz, 1 H, bridging hydrido) ppm. ^{31}P NMR (300 MHz, CD_2Cl_2, 27 °C): δ = –0.70 (d, $J_{P,P}$ = 16.7 Hz, 1 P), –1.22 (d, $J_{P,P}$ = 16.7 Hz, 1 P) ppm. ^{31}P NMR (300 MHz, CD_2Cl_2, –90 °C): δ = 1.27 (d, $J_{P,P}$ = 16.8 Hz, 1 P), –0.36 (d, $J_{P,P}$ = 16.8 Hz, 1 P), –0.69 (d, $J_{P,P}$ = 16.5 Hz, 1 P), –2.13 (d, $J_{P,P}$ = 16.4 Hz, 1 P) ppm. ^{1}H-^{187}Os 2D HMQC NMR (600 MHz, CD_2Cl_2, –100 °C): δ = –13965 ($^1J_{Os,P}$ = 147 Hz), –13230 ($^1J_{Os,P}$ = 211 Hz) ppm.

7: $C_{54}H_{39}O_6Os_3P_3S_3$ (1543.69). FAB-MS: *m/z* = 1544 [M$^+$], 1516 [M$^+$ – CO], 1488 [M$^+$ – 2 CO], 1460 [M$^+$ – 3 CO]. IR (CH_2Cl_2): $\tilde{\nu}_{co}$ = 2068 w, 2058 w, 2025 sh, 2015 m, 1985 s, 1961 sh, 1929 sh cm^{-1}. ^{1}H NMR (300 MHz, $CDCl_3$, 20 °C): δ = 7.85–6.65 (m, 38 H, arom.), –16.67 [t, $J_{H,P}$ = 11 Hz, 1 H, bridging hydrido] ppm. ^{31}P NMR (300 MHz, $CDCl_3$, 20 °C): δ = 4.50 (m, 1 P), –1.65 (d, *J* = 16.18 Hz, 1 P), –5.98 (m, 1 P) ppm.

8: $C_{55}H_{39}O_7Os_3P_3S_3$ (1571.7). FAB-MS: *m/z* = 1572 [M$^+$], 1544 [M$^+$ – CO]. IR (CH_2Cl_2): $\tilde{\nu}_{co}$ = 2061 m, 2040 vs, 2002 s, 1988 m, 1968 w, 1944 m cm^{-1}. ^{1}H NMR (300 MHz, $CDCl_3$, 20 °C): δ = 7.85–6.20 (m, 38 H, arom.), –17.05 [t (dd), $J_{H,P}$ = 14.7 Hz, $J_{H,P}$ = 13.2 Hz, 1 H, bridging hydrido] ppm. ^{1}H NMR (300 MHz, CD_2Cl_2, –50 °C, hydrido region): δ = –17.16 (t, *J* = 13.5 Hz, 12.9 Hz, 1 H) ppm. ^{31}P NMR (300 MHz, $CDCl_3$, 20 °C): δ = –3.19 (m), –5.30 (d, *J* = 17.1 Hz), –9.15 (m) ppm. ^{31}P NMR (300 MHz, CD_2Cl_2, –35 °C): δ = –0.58 (d, *J* = 9.95 Hz, 1 P), –9.5 (2, 1 P), –11.15 (s, 1 P) ppm.

X-ray Crystallographic Study: Crystals of **2**, **3**, **5** and **6** were obtained by slow concentration of dichloromethane/*n*-hexane solu-

Table 5. Crystal data and experimental details for $[Os_3(CO)_{10}\{Ph_2P(C_4H_3S)\}_2]$ (**2**); $[Os_3(CO)_9\{Ph_2P(C_4H_3S)\}_3]$ (**3**); $[(\mu\text{-}H)Os_3(CO)_9\{\mu_3\text{-}Ph_2P(C_4H_2S)\}]$ (**5**); $[(\mu\text{-}H)Os_3(CO)_8\{\mu_3\text{-}Ph_2P(C_4H_2S)\}\{Ph_2P(C_4H_3S)\}]$(**6**).

	2	**3**	**5**$\cdot 0.5C_6H_{14}$	**6**
Empirical formula	$C_{42}H_{26}O_{10}Os_3P_2S_2$	$C_{57}H_{42}O_9Os_3P_3S_3$	$C_{25}H_{13}O_9Os_3PS\cdot 0.5C_6H_{14}$	$C_{40}H_{26}O_8Os_3P_2S_2$
Formula mass	1387.29	1630.60	1112.53	1331.27
T [K]	293(2)	293(2)	293(2)	293(2)
λ [Å]	0.71069	0.71069	0.71069	0.71069
Crystal system	triclinic	triclinic	triclinic	orthorhombic
Space group	$P\bar{1}$ (no. 2)	$P\bar{1}$ (no. 2)	$P\bar{1}$ (no. 2)	$P2_12_12_1$ (no. 19)
a [Å]	12.461(2)	14.067(2)	13.474(3)	10.846(4)
b [Å]	12.857(4)	18.872(5)	13.669(2)	14.370(3)
c [Å]	14.180(5)	25.004(3)	17.309(5)	25.455(4)
α [°]	70.69(2)	70.26(2)	85.68(2)	90
β [°]	79.12(2)	75.08(2)	77.86(2)	90
γ [°]	88.55(2)	86.97(2)	74.05(1)	90
V [Å^3]	2103.8(9)	6033(2)	2996(1)	3967(2)
Z	2	4	4	4
$D_{\text{calcd.}}$ [Mg·m^{-3}]	2.190	1.795	2.466	2.229
μ(Mo-K_α) [mm^{-1}]	9.270	6.537	12.863	9.822
F(000)	1296	3108	2026	2480
Crystal size [mm]	0.35 × 0.24 × 0.20	0.25 × 0.11 × 0.08	0.27 × 0.25 × 0.20	0.30 × 0.25 × 0.22
θ limits [°]	2–27	2–25	2–27	2–27
Reflections collected	9104 ($\pm h$, $\pm k$, $+l$)	21091 ($\pm h$, $\pm k$, $+l$)	13008 ($\pm h$, $\pm k$, $+l$)	4801($+h$, $+k$, $+l$)
Unique observed reflections [$I > 2\sigma(I)$]	6941	8123	8000	4062
Goodness of fit (F^2)	1.033	0.933	0.989	1.063
R_1 (F)[a], wR_2 (F^2)[b] [$I > 2\sigma(I)$]	0.0268, 0.0683	0.0766, 0.1544	0.0441, 0.1081	0.0249, 0.0601
Absolute structure parameter	–	–	–	–0.02(1)
Largest diff. peak/hole [e·Å^{-3}]	1.340/–0.989	2.055/–2.330	2.204/–2.184	0.925/–0.963

[a] $R_1 = \Sigma||F_o| - |F_c||/\Sigma|F_o|$. [b] $wR_2 = [\Sigma w(F_o{}^2 - F_c{}^2)^2/\Sigma w(F_o{}^2)^2]^{1/2}$, $w = 1/[\sigma^2(F_o{}^2) + (aP)^2 + bP]$, $P = (F_o{}^2 + 2F_c{}^2)/3$.

tions at 4 °C. Crystal data and other experimental details for all structures are reported in Table 5. The diffraction experiments were carried out with an Enraf–Nonius CAD4 diffractometer at room temperature, using graphite-monochromatized Mo-K_α radiation (λ = 0.71073 Å). The unit cells were determined by a least-squares fitting procedure using 25 randomly selected strong reflections. The diffracted intensities were corrected for Lorentz and polarisation effects. An empirical absorption correction was applied using the azimuthal scan method.[51] The positions of the metal atoms were determined by direct methods (SIR-97[52]) and all non-hydrogen atoms were located from Fourier difference syntheses. In compounds **5** and **6**, the bridging hydrido ligands were also located in the Fourier map. The phenyl and thienyl H atoms were added in calculated positions ($d_{\text{C–H}}$ 0.93 Å). The final refinement on F^2 proceeded by full-matrix least-squares calculations (SHELXL97[53]) using anisotropic thermal parameters for all non-hydrogen atoms in **2**, **5** and **6**, whereas in **3** only the Os, P and S atoms were treated anisotropically. The asymmetric units of **3** and **5** contain two independent molecules, and the latter contains also one-half of a disordered *n*-hexane solvent molecule, which is related to the other half by an inversion centre. The 2-thienyl rings [bound to P(4) and P(5), respectively] of one of the molecules present in the asymmetric unit of **3** showed disorder due to a 180° rotation around the P–C axis, and therefore the sulfur and α-carbon atoms of the rings were refined for the two orientations. The refined occupancy factors of S(4) and S(5) in the second conformer of the molecule (Figure S3, Supporting Information) were 52 and 66%, respectively. The phenyl and thienyl H atoms were assigned isotropic thermal parameters 1.2 times U_{eq} of the carrier carbon atoms. The relatively low quality of the diffraction data for compound **3** was due to the fact that good quality crystals could not be obtained despite repeated crystallisations by different techniques. CCDC-203202 (**2**), -203203 (**3**), -203204 (**5**) and -203205 (**6**) contain the supplementary crystallographic data for this paper. These data can be obtained free of charge from The Cambridge Crystallographic Data Centre via www.ccdc.cam.ac.uk/data_request/cif.

Acknowledgments

This research was supported by grants to E. N. from the Swedish Research Council (VR) and the European Union (TMR network Metal Clusters in Catalysis and Organic Synthesis, MECATSYN). We would like to thank Dr. Jason D. King for his helpful comments on the variable-temperature NMR spectra, and Prof. Silvio Aime and Dr. Karl-Erik Bergquist for the use of NMR spectrometers. M. M. and S. S. thank the University of Bologna and MIUR (Cofin2003) for financial support.

---

[1] H. Topsøe, B. S. Claussen, F. E. Massoth, "Hydrotreating Catalysis", in: *Catalysis*: *Science and Technology* (Eds.: J. R. Anderson, M. Boudart), Springer-Verlag, New York, **1996**, vol. 11.
[2] D. G. Churchill, B. M. Bridgewater, G. Parkin, *J. Am. Chem. Soc.* **2000**, *122*, 178.
[3] C. Bianchini, A. Meli, *Acc. Chem. Res.* **1998**, *31*, 109.
[4] R. J. Angelici, *Acc. Chem. Res.* **1988**, *21*, 387.
[5] N. N. Sauer, R. J. Angelici, *J. Catal.* **1989**, *116*, 11.
[6] R. J. Angelici, *Polyhedron* **1997**, *16*, 3073.
[7] M. Brorson, J. D. King, K. Kiriakidou, F. Prestopino, E. Nordlander, *Metal Clusters in Chemistry* (Eds.: P. Braunstein, L. A. Oro, P. R. Raithby), Wiley-VCH, Weinheim, **1999**, vol. 2, chapter 2.6, pp. 741–781.
[8] H. D. Kaesz, R. B. King, T. A. Manuel, L. D. Nichols, F. G. A. Stone, *J. Am. Chem. Soc.* **1960**, *82*, 4749.
[9] R. B. King, P. M. Treichel, F. G. A. Stone, *J. Am. Chem. Soc.* **1961**, *83*, 3600; R. B. King, F. G. A. Stone, *J. Am. Chem. Soc.* **1961**, *82*, 4557.
[10] A. E. Ogilvy, M. Draganjac, T. B. Rauchfuss, S. R. Wilson, *Organometallics* **1988**, *7*, 1171.

[11] A. J. Arce, P. Arrojo, A. J. Deeming, Y. De Sanctis, *J. Chem. Soc., Dalton Trans.* **1992**, 2423.

[12] M. A. Reynolds, I. A. Guzei, R. J. Angelici, *Chem. Commun.* **2000**, 513; M. A. Reynolds, I. A. Guzei, R. J. Angelici, *J. Am. Chem. Soc.* **2002**, *124*, 513.

[13] A. J. Arce, J. Manzur, M. Márquez, Y. De Sanctis, A. J. Deeming, *J. Organomet. Chem.* **1991**, *412*, 177.

[14] A. J. Arce, A. J. Deeming, Y. De Sanctis, R. Marchado, J. Manzur, C. Rivas, *J. Chem. Soc., Chem. Commun.* **1990**, 1568.

[15] M. W. Day, K. I. Hardcastle, A. J. Deeming, A. J. Arce, Y. De Sanctis, *Organometallics* **1990**, *9*, 6.

[16] A. J. Arce, P. Arrojo, Y. De Sanctis, M. Márquez, A. J. Deeming, *J. Organomet. Chem.* **1994**, *479*, 159.

[17] A. J. Arce, A. Karam, Y. De Sanctis, M. V. Capparelli, A. J. Deeming, *Inorg. Chim. Acta* **1999**, *285*, 277.

[18] J. D. King, M. Monari, E. Nordlander, *J. Organomet. Chem.* **1999**, *573*, 272.

[19] A. J. Deeming, M. K. Shinhmar, A. J. Arce, Y. De Sanctis, *J. Chem. Soc., Dalton Trans.* **1999**, 1153.

[20] A. J. Deeming, S. N. Jayasuriya, A. J. Arce, Y. De Sanctis, *Organometallics* **1996**, *15*, 786.

[21] M. I. Bruce, B. K. Nicholson, M. L. Williams, *J. Organomet. Chem.* **1983**, *243*, 69.

[22] M. I. Bruce, J. G. Matisons, B. K. Nicholson, *J. Organomet. Chem.* **1983**, *247*, 321.

[23] M. I. Bruce, M. L. Williams, B. K. Nicholson, *J. Organomet. Chem.* **1983**, *258*, 63.

[24] K. Biradha, V. M. Hansen, W. K. Leong, R. K. Pomeroy, M. J. Zaworotko, *J. Cluster Sci.* **2000**, *11*, 285.

[25] R. F. Alex, R. K. Pomeroy, *Organometallics* **1987**, *6*, 2437.

[26] A. J. Deeming, S. Donovan-Mtunzi, S. E. Kabir, P. J. Maning, *J. Chem. Soc., Dalton Trans.* **1985**, 1037.

[27] W. K. Leong, Y. Liu, *J. Organomet. Chem.* **1999**, *584*, 174.

[28] M. R. Churchill, B. G. Deboer, *Inorg. Chem.* **1977**, *16*, 878.

[29] M. I. Bruce, M. J. Liddell, C. A. Hughes, J. M. Patrick, B. W. Skelton, A. H. White, *J. Organomet. Chem.* **1988**, *347*, 157.

[30] V. M. Hansen, A. K. Ma, K. Biradha, R. K. Pomeroy, M. J. Zaworotko, *Organometallics* **1998**, *17*, 5267.

[31] M. I. Bruce, M. J. Liddell, C. A. Hughes, J. M. Patrick, B. W. Skelton, A. H. White, *J. Organomet. Chem.* **1988**, *347*, 181.

[32] M. I. Bruce, M. J. Liddell, O. Shawkataly, C. A. Hughes, B. W. Skelton, A. H. White, *J. Organomet. Chem.* **1988**, *347*, 207.

[33] A. J. Deeming, S. Hasso, *J. Organomet. Chem.* **1975**, *88*, C21.

[34] B. F. G. Johnson, J. Lewis, E. Nordlander, P. R. Raithby, *J. Chem. Soc., Dalton Trans.* **1996**, 3825.

[35] S. Aime, R. Gobetto, E. Valls, *Inorg. Chim. Acta* **1998**, *521*, 275–276.

[36] M. A. Gallop, B. F. G. Johnson, J. Lewis, *J. Chem. Soc., Chem. Commun.* **1987**, 1831.

[37] R. Benn, in: *Transition Metal Nuclear Magnetic Resonance* (Ed.: P. S. Pregosin), Elsevier, Amsterdam, **1991**.

[38] A. E. Aliev, A. J. Deeming, M. J. Stchedroff, J. W. Steed, unpublished results.

[39] M. J. Stchedroff, S. Aime, R. Gobetto, L. Salassa, E. Nordlander, *Magn. Reson. Chem.* **2002**, *40*, 107.

[40] J. D King, J. E. Davies, M. H. Johansson, B. F. G. Johnson, E. Nordlander, unpublished results.

[41] A. J. Deeming, S. E. Kabir, N. J. Powell, P. A. Bates, M. B. Hursthouse, *J. Chem. Soc., Dalton Trans.* **1987**, 1529.

[42] A. J. Arce, A. J. Deeming, Y. De Sanctis, D. M. Speel, A. Di Trapani, *J. Organomet. Chem.* **1999**, *580*, 370.

[43] R. Gobetto, E. Sappa, A. Tiripicchio, M. Tiripicchio Camellini, M. J. Mays, *J. Chem. Soc., Dalton Trans.* **1990**, 807.

[44] N. K. Kiriakidou Kazemifar, M. J. Stchedroff, M. A. Mottalib, M. H. Johansson, M. Monari, S. Selva, E. Nordlander, unpublished results.

[45] S. P. Tunik, I. O. Koshevoy, A. J. Poe, D. H. Farrar, E. Nordlander, T. A. Pakkanen, M. Haukka, *Dalton Trans.* **2003**, 2457.

[46] A. J. Deeming, S. Hasso, *J. Organomet. Chem.* **1976**, *114*, 313.

[47] S. R. Drake, P. Loveday, *Inorg. Synth.* **1990**, *28*, 230.

[48] H. D. Kaesz, S. A. R. Knox, J. W. Koepke, R. B. Saillant, *J. Chem. Soc. D* **1971**, 477.

[49] A. J. Deeming, S. Hasso, M. Underhill, *J. Chem. Soc., Dalton Trans.* **1975**, 1614.

[50] B. F. G. Johnson, J. Lewis, P. Kilty, *J. Chem. Soc. A* **1968**, 2859.

[51] A. C. T. North, D. C. Philips, F. S. Mathews, *Acta Crystallogr., Sect. A* **1968**, *24*, 351.

[52] A. Altomare, M. C. Burla, M. Camalli, G. L. Cascarano, C. Giacovazzo, A. Guagliardi, A. G. G. Moliterni, G. Polidori, R. Spagna, *J. Appl. Crystallogr.* **1999**, *32*, 115.

[53] G. M. Sheldrick, *SHELXL-97, Program for crystal structure refinement*, University of Göttingen, Germany, **1997**.

Received: December 22, 2005